Propagation Characteristics of Coplanar-Type Transmission Lines with Lossy Media

Toshihide Kitazawa, *Senior Member, IEEE*, and Tatsuo Itoh, *Fellow, IEEE*

Abstract—**Lossy coplanar-type transmission lines are analyzed based on the hybrid-mode formulation by combining the spectral-domain approach with the perturbation method. Introducing a finite thickness of metallization and choosing the proper basis functions for the thick conductor model prevent the integrals used for calculating the conductor losses from becoming singular when evaluated at the conductor edge. Also, advantage is taken of an orthogonality relation which is used to reduce the double infinite or semi-infinite integral to a single integral, thus reducing the computation labor drastically. Numerical computations by new basis functions for the thick conductor show convergence rates as fast as those for the zero-thickness cases. Numerical results include the effective dielectric constants, characteristic impedances, and total losses (conductor and dielectric losses) for slot lines and symmetrical and asymmetrical coplanar waveguides.**

I. Introduction

THE usefulness of coplanar-type transmission lines, e.g., slot lines and coplanar waveguide (CPW), is increasing at higher microwave and millimeter-wave frequencies. At these frequencies, the performance quality of microstrip lines deteriorates because via holes are required for shunt element connections. Miniaturization at higher frequencies requires accurate analyses for the propagation characteristics. Propagation characteristics, such as phase constants and characteristic impedances, of lossless coplanar-type transmission lines have been investigated extensively based on the quasi-static [1]–[13] as well as the hybrid-mode formulation [2], [4], [5]. In these transmission lines, the metallization thickness effect, in general, is larger than that of striplines because of the field configurations [5]–[7]; thus analytical methods ought to take this effect into consideration. For the lossy transmission line case, attenuation should be evaluated in addition to the phase constants and characteristic impedances [8]. Most frequency-dependent loss calculations have been based on the perturbational scheme with the assumptions that the metallization thickness is zero as well as sufficiently greater than the skin depth [9], [10]. These loss power calculations require evaluation of either double infinite or semi-infinite integrals. However, calculations based on a zero-thickness conductor cause a computational difficulty, in which the power lost in the conductor is not principally integrable [11]. The integrand contains a pole of first order owing to the $\delta^{-1/2}$ variation of the field near the conductor edge, where δ is the distance from the edge. To avoid a logarithmic divergence, the integrals are terminated at a definite distance just short of the edge. This termination point is usually determined by the conductor thickness only [9], but it should depend on other parameters, such as the line width and the dielectric constant.

In this paper, the spectral-domain approach [12], [13] is extended to analyze coplanar-type transmission lines with finite metallization thickness, and the perturbation

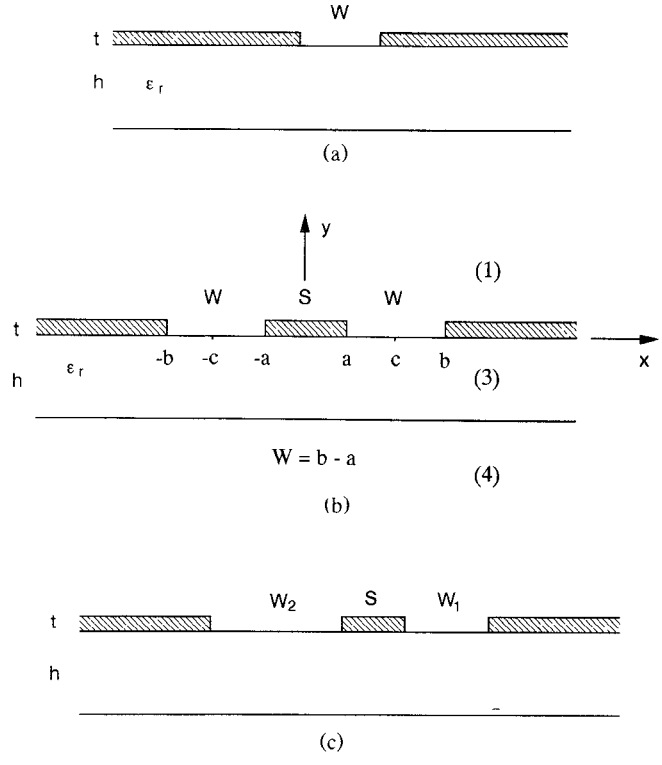

Fig. 1. Coplanar-type transmission lines: (a) slot line; (b) symmetrical coplanar waveguide; (c) asymmetrical coplanar waveguide.

Manuscript received August 30, 1990; revised May 1, 1991. This work was supported in part by the Office of Naval Research under Grant N00014-89-J-1006.

T. Kitazawa was with the Department of Electronic Engineering, Kitami Institute of Technology, Kitami, 090 Japan. He is now with the Department of Electrical Engineering, Ibaraki University, Hitachi, 316 Japan.

T. Itoh is with the Department of Electrical Engineering, University of California at Los Angeles, Los Angeles, CA 90024.

IEEE Log Number 9102338.

method is introduced to evaluate losses taking the metallization thickness effect into consideration. Introducing the finite metallization model and choosing the proper basis functions for the model make the integral remain finite up to the conductor edge $\delta = 0$. Also, the use of the orthogonality relation of the modes reduces the double infinite or semi-infinite integral for the loss-power calculation to a single integral, thereby reducing the computation labor drastically.

II. Hybrid-Mode Formulation Procedure of Electromagnetic Field

The formulation procedure for the lossless case is based on the extended spectral-domain approach. It has been presented in [13] and is explained here only briefly for the symmetrical CPW shown in Fig. 1(b). The numerical results for slot lines (Fig. 1(a)) and asymmetrical CPW (Fig. 1(c)) will be presented later. Losses are assumed small and will be accounted for by the perturbational scheme which follows. Electromagnetic fields in the open regions ($y > t$, $y < 0$) are expressed by the Fourier integral representation in the x direction in the form

$$E_x^{(m)}(x,y,z) = \frac{1}{\sqrt{2\pi}} \int_{-\infty}^{\infty} \tilde{E}_x^{(m)}(y) e^{-j\alpha x} d\alpha : e^{-j\beta z} \quad (m = 1,3,4) \tag{1}$$

while fields in the aperture region ($t > y > 0$) are expressed by the Fourier series representation with respect to the x direction as

$$E_x^{(2)}(x,y,z) = \frac{1}{\sqrt{2W}} \sum_{n=-\infty}^{\infty} \tilde{E}_x^{(2)}(y) e^{-j\alpha_n (x-c)} e^{-j\beta z} \tag{2}$$

where β is the phase constant, c represents the center of the aperture, and the Fourier variables, α_n, in the aperture region are determined so that the boundary conditions at the conductors are satisfied.

$$\alpha_n = \frac{n\pi}{W}. \tag{3}$$

Applying the continuity conditions at the interface at $y = -h$ and introducing the aperture fields at $y = t$, $e^U(x)$ and at $y = 0$, $e^L(x)$, the electromagnetic fields in the subregions can be related to the aperture fields $e^U(x)$ and $e^L(x)$ [13]:

$$E^{(m)}(x,y,z) = \int_{x'} \int_{\alpha} \left\{ \bar{\bar{T}}_U^{(m)}(\alpha; x, y|x') e^U(x') + \bar{\bar{T}}_L^{(m)}(\alpha; x, y|x') e^L(x') \right\} d\alpha\, dx'\, e^{-j\beta z} \tag{4}$$

$$H^{(m)}(x,y,z) = \int_{x'} \int_{\alpha} \left\{ \bar{\bar{Y}}_U^{(m)}(\alpha; x, y|x') e^U(x') + \bar{\bar{Y}}_L^{(m)}(\alpha; x, y|x') e^L(x') \right\} d\alpha\, dx'\, e^{-j\beta z} \tag{5}$$

$$E^{(2)}(x,y,z) = \int_{x'} \sum_{n} \left\{ \bar{\bar{T}}_U^{(2)}(n; x, y|x') e^U(x') + \bar{\bar{T}}_L^{(2)}(n; x, y|x') e^L(x') \right\} dx'\, e^{-j\beta z} \tag{6}$$

$$H^{(2)}(x,y,z) = \int_{x'} \sum_{n} \left\{ \bar{\bar{Y}}_U^{(2)}(n; x, y|x') e^U(x') + \bar{\bar{Y}}_L^{(2)}(n; x, y|x') e^L(x') \right\} dx'\, e^{-j\beta z} \tag{7}$$

where the $\bar{\bar{T}}$'s and $\bar{\bar{Y}}$'s are dyadic Green's functions.

III. Propagation Parameters for Lossless Cases

Applying the remaining boundary conditions (continuities of the magnetic fields at the aperture surface $y = t$ and 0) to (5) and (7), we obtain the integral equations for the aperture fields $e^U(x)$ and $e^L(x)$ and, implicitly, the phase constant β. Then, applying Galerkin's procedure [2], [12], [13] to the integral equations, we obtain the determinantal equation for β. The phase constant β is, in turn, substituted into (4)–(7) to obtain the electromagnetic fields in each region. Then, characteristic impedances are calculated by using these fields. The frequency-dependent characteristic impedance is not uniquely specified for the hybrid-mode propagation, and possible definitions are [2], [7], [10], [13]

$$\text{power–voltage basis:} \quad Z_{PV} = \frac{V_0^2}{P_0} \tag{8}$$

$$\text{power–current basis:} \quad Z_{PI} = \frac{P_0}{I_0^2} \tag{9}$$

$$\text{voltage–current basis:} \quad Z_{VI} = \frac{V_0}{I_0} \tag{10}$$

where V_0 and I_0 are the voltage difference between conductors and the total current on the signal conductor, respectively. P_0 is the average power flow in the z direction, and it can be given by

$$P_0 = \frac{1}{2} \operatorname{Re} \left(\int_S \boldsymbol{E} \times \boldsymbol{H}^* \cdot \boldsymbol{n}_z \, dS \right). \tag{11}$$

Numerical computations and a discussion of impedances based on these definitions are included in a later section.

IV. Basis Functions

In Galerkin's procedure, the unknown aperture fields $e^U(x)$ and $e^L(x)$ are expanded in terms of the appropriate basis functions:

$$e_x^U(x') = \sum_{k=1}^{N_x} a_{xk} f_{xk}(x) \qquad e_x^L(x') = \sum_{k=1}^{N_x} b_{xk} f_{xk}(x)$$

$$e_z^U(x') = \sum_{k=1}^{N_z} a_{zk} f_{zk}(x) \qquad e_z^L(x') = \sum_{k=1}^{N_z} b_{zk} f_{zk}(x). \tag{12}$$

For coplanar types of transmission line, such as slot lines and coplanar waveguides, with metallizations of zero thickness, the fields have a $\delta^{-1/2}$ variation near the edge [14]. Taking this edge effect into consideration, the following basis functions have been proposed [2], [5]:

$$f_{xk}(x)=\frac{T_k\left\{\dfrac{2(x-c)}{W}\right\}}{\sqrt{1-\left\{\dfrac{2(x-c)}{W}\right\}^2}} \qquad f_{zk}(x)=U_k\left\{\frac{2(x-c)}{W}\right\} \tag{13}$$

where $T_k(x)$ and $U_k(x)$ are Chebyshev polynomials of the first and the second kind, respectively. This set of basis functions gives fast convergence, and accurate results have been obtained for a small number of basis functions for lossless cases [2], [5]. This set of basis functions has also been used for planar transmission lines with finite metallization thickness, and reasonable results have been obtained for phase constants and characteristic impedance calculations [6], [7]. However, when the fields expressed in terms of this set of basis functions are used to calculate conductor loss by the perturbation scheme, the resulting integrand contains a pole of the first order at the edge [11]. To avoid this divergence, the following basis functions are used in the computations here:

$$f_{xk}(x)=\left[1-\left\{\frac{2(x-c)}{W}\right\}^2\right]^{-1/3} C_{2k}^{1/6}\left\{\frac{2(x-c)}{W}\right\}$$

$$f_{zk}(x)=\left[1-\left\{\frac{2(x-c)}{W}\right\}^2\right]^{2/3} C_{2k-1}^{7/6}\left\{\frac{2(x-c)}{W}\right\} \tag{14}$$

where $C_k^{\mu}(x)$ are Gegenbauer polynomials. The basis functions in (14) represent the actual field variations more properly near the edge of a conductor of finite thickness by exhibiting $\delta^{-1/3}$ variations for the transverse components of electric fields and $\delta^{2/3}$ for the longitudinal components of electric fields [14].

V. Perturbation Formula for Lossy Cases

Attenuation caused by imperfect conductors and dielectrics is accounted for by the perturbational procedure. Loss caused by the imperfect conductor is determined by

$$\alpha_c=\frac{P_C}{2P_0} \tag{15}$$

The average power flow, P_0, is given by (11) and the power lost in the conductors, P_C, is given by

$$P_C=\frac{1}{2}R_s\int_C|\boldsymbol{H}_t|^2\,dl \tag{16}$$

where H_t is the tangential component of the magnetic field on the conductor surface, C, in the lossless case. Conventional methods [10] have neglected the metal conductor thickness and used a set of basis functions which have a $\delta^{-1/2}$ variation near the edge, which produces a divergence when the integrals of (16) are performed up to the edge. To avoid this divergence, the integrals were terminated at a definite distance just short of the edge [9], [10]. The magnetic field grows rapidly near the edge, so the determination of the truncation point has a pronounced effect on the value of the loss power. However, the termination point was determined simply by the conductor thickness only ($\delta=t/270$) [9], [10], while it ought to depend on other parameters, such as the center strip width and the dielectric constant. In this paper, we take the conductor thickness into consideration and use appropriate basis functions, which have a $\delta^{-1/3}$ variation (14) instead of the $\delta^{-1/2}$ variation of the zero-thickness cases. The integrals can be evaluated numerically up to the conductor edge at $\delta=0$. However a direct evaluation of the integration (16) should be avoided, because it requires the semi-infinite x integral of the infinite α integral in (5) and (7). Instead, we rewrite the contour integral (16) as

$$\begin{aligned}\int_C|\boldsymbol{H}_t|^2\,dl=&\int_{-\infty}^{\infty}|\boldsymbol{H}_t(t+0)|^2\,dx-2\int_a^b|\boldsymbol{H}_t(t-0)|^2\,dx\\&+\int_{-\infty}^{\infty}|\boldsymbol{H}_t(-0)|^2\,dx-2\int_a^b|\boldsymbol{H}_t(+0)|^2\,dx\\&+2\int_0^t|\boldsymbol{H}_t(x=a)|^2\,dz+2\int_0^t|\boldsymbol{H}_t(x=b)|^2\,dz.\end{aligned} \tag{17}$$

Substituting (5) into (17) and utilizing the orthogonality relation of the modes in each region, the first four integrals on the right-hand side reduce to the single α integrals, and only the remaining two y integrals are evaluated numerically over the small interval t. This procedure drastically reduces the computational labor required for the conductor loss calculation (double integrals become

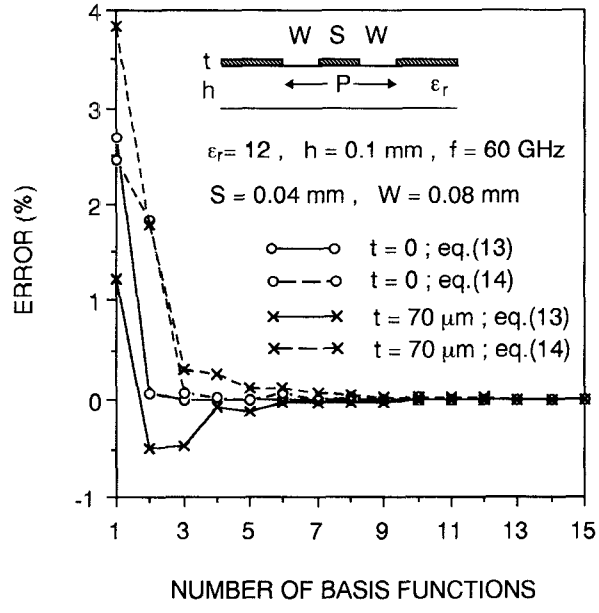

Fig. 2. Convergence of calculated results using two different sets of basis functions.

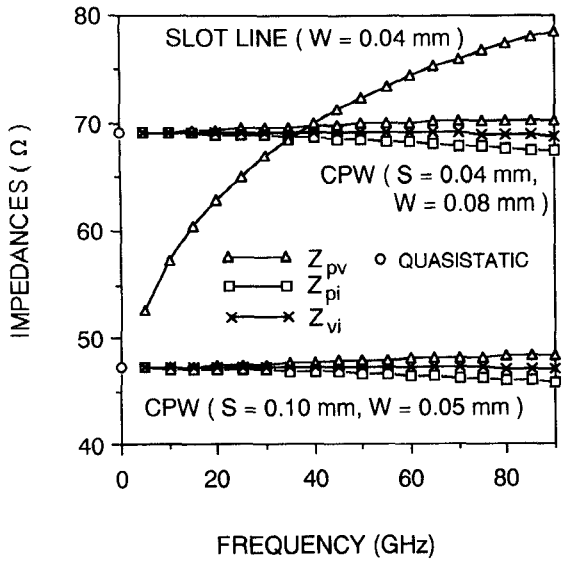

Fig. 3. Characteristic impedances of slot line and symmetrical coplanar waveguide based on different definitions.

single integrals). If the integrals are terminated at some point near the edge to avoid the divergence, then the orthogonality relation can not longer be utilized. It not only reduces the accuracy but also requires significantly more computation time.

Loss caused by imperfect dielectric is determined by

$$\alpha_d = \frac{P_d}{2P_0}. \tag{18}$$

The power lost in the dielectric, P_d, is given by

$$P_d = \frac{1}{2}\omega\epsilon \tan\delta \int_{S_d} |E|^2 \, dS \tag{19}$$

where S_d stands for the region occupied by the dielectric media, and E is the electric field for the lossless case.

VI. Results

Preliminary computations have been carried out to show the validity of the basis functions used in the present method. Fig. 2 shows the convergence of the calculated results with respect to the number of basis functions for symmetrical CPW. Two sets of basis functions from (13) and (14) are used to calculate the effective dielectric constants, defined as

$$\epsilon_{\text{eff}} = \left(\beta / \omega\sqrt{\epsilon_0\mu_0}\right)^2 \tag{20}$$

for both zero ($t = 0$) and finite ($t \neq 0$) metallization thicknesses. The number of basis functions is increased to $N = 15$ for each case, and the percentage error for the $N = 15$ case is shown. Rapid convergence is observed for both zero and finite-thickness cases by using (13) or (14). Similar convergence has been observed for the calculation of the characteristic impedances defined in (8)–(10). Accurate values for P_0 and V_0 in (8)–(10) can be obtained easily. The total current, I_0, on the center strip, $-a < x < a$, is evaluated by

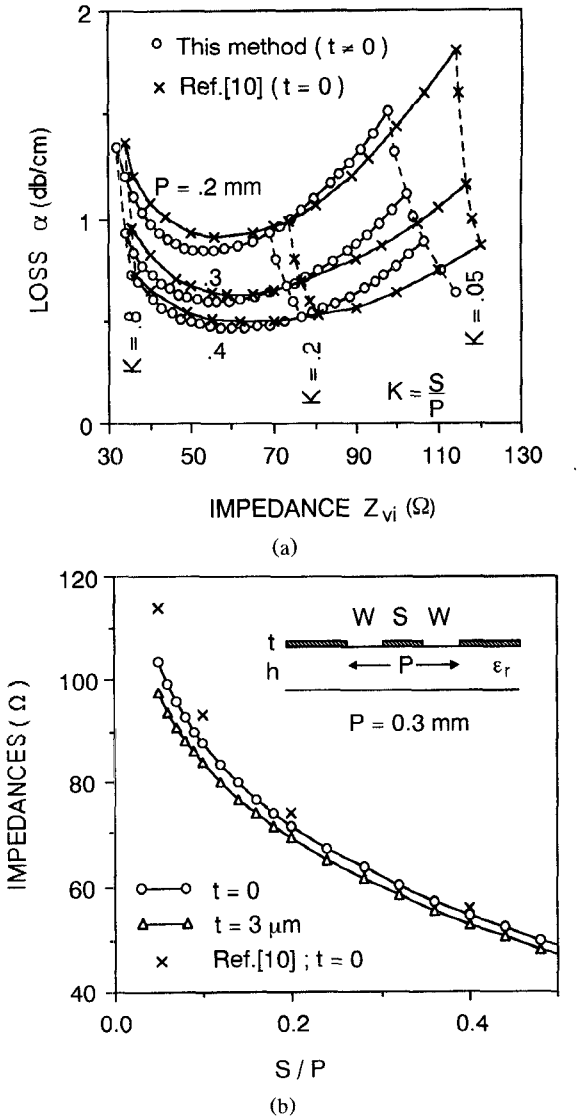

Fig. 4. Propagation characteristics of symmetrical coplanar waveguide: (a) attenuation constant; (b) comparison of characteristic impedances. Dielectrics: $\epsilon_r = 12.8$, $\tan\delta = 0.0006$, $h = 0.1$ mm. Conductor: $\rho = 1.7$ $\mu\Omega\cdot$cm, $t = 3$ μm.

$$I_0 = \int_{-a}^{a} \left\{H_x^{(3)}(x, y = -0) - H_x^{(1)}(x, y = t + 0)\right\} dx + \int_0^t \left\{H_y^{(2)}(x = a, y) - H_y^{(2)}(x = -a, y)\right\} dy \tag{21}$$

but the value I_0 obtained by substituting (5) and (7) into (21) is somewhat lacking in rigor, for it is relatively sensitive to variations in aperture fields. The expression for I_0 that will be derived next is insensitive to variations in the aperture fields and provides more accurate results with a smaller number of basis functions, N. The total current on the center strip can be expressed as

$$I_0 = I(x_1) = \int_{-x_1}^{x_1} \left\{H_x^{(3)}(x, y = -0) - H_x^{(1)}(x, y = t + 0)\right\} dx + \int_0^t \left\{H_y^{(2)}(x = x_1, y) - H_y^{(2)}(x = -x_1, y)\right\} dy \tag{22}$$

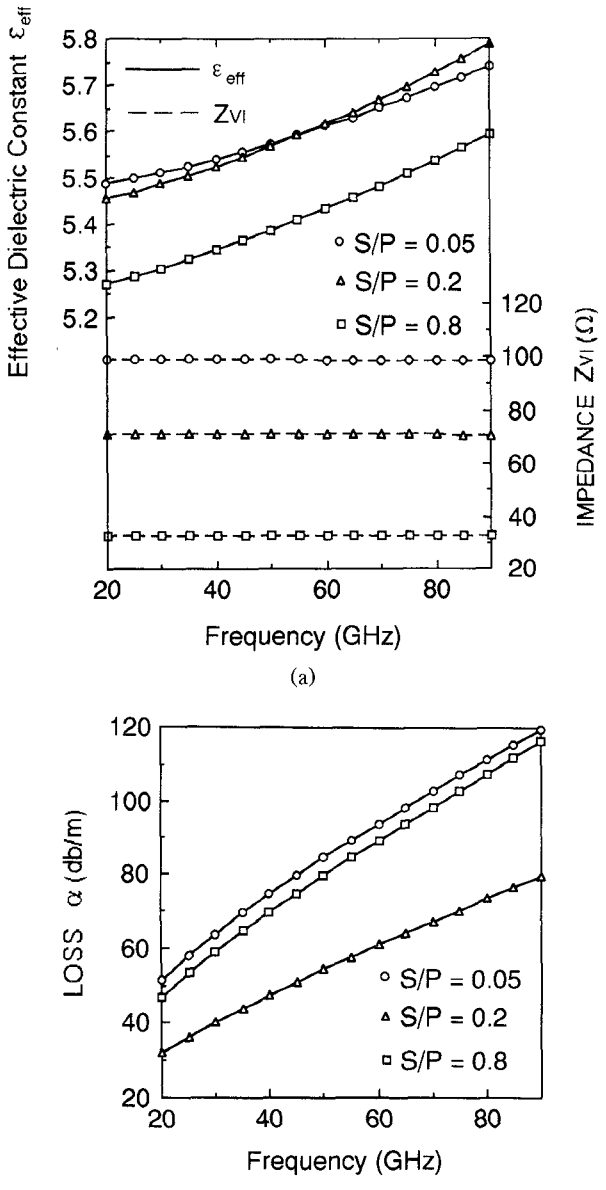

Fig. 5. Propagation characteristics of symmetrical coplanar waveguide: (a) effective dielectric constant and characteristic impedance; (b) attenuation constant. Dielectrics: $\epsilon_r = 12.8$, $\tan\delta = 0.0006$, $h = 0.1$ mm. Conductor: $\rho = 1.7\ \mu\Omega\cdot$cm, $t = 6\ \mu$m, $P = 0.3$ mm.

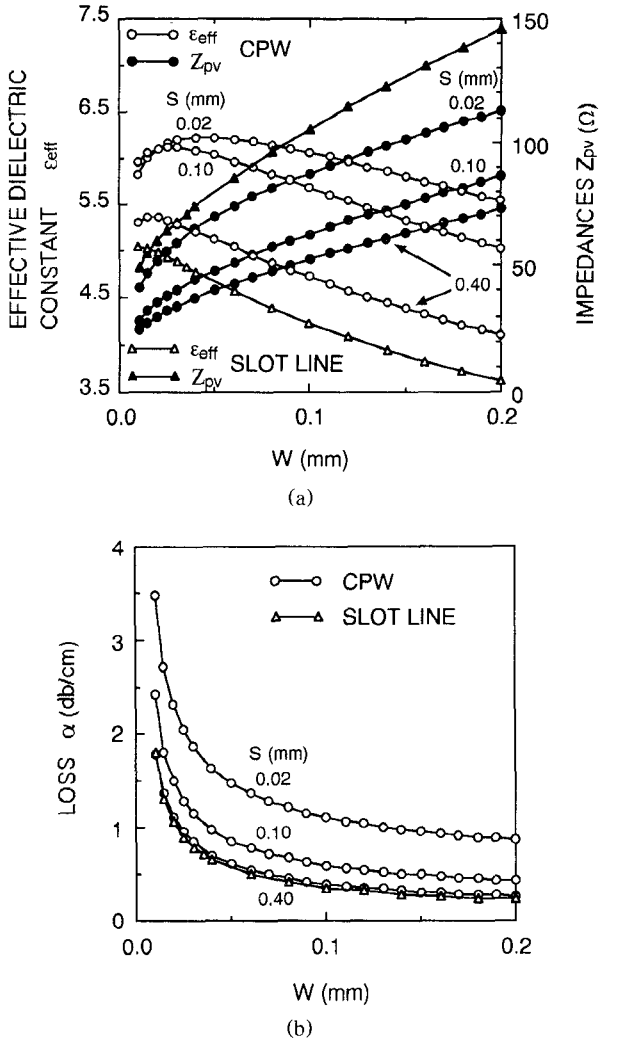

Fig. 6. Propagation characteristics of slot line and symmetrical coplanar waveguide: (a) effective dielectric constant, and characteristic impedance of lossless care; (b) attenuation constant. Dielectrics: $\epsilon_r = 12.8$, $\tan\delta = 0.0006$, $h = 0.1$ mm. Conductor: $\rho = 1.7\ \mu\Omega\cdot$cm, $t = 3\ \mu$m. $f = 60$ GHz.

where x_1 lies within the right aperture, $a < x_1 < b$. Multiplying (22) by $e^U(x_1)$ and integrating over the right aperture, $a < x_1 < b$, we obtain

$$I_0 = \int_a^b e_x^U(x_1)\, I(x_1)\, dx_1 \left\{ \int_a^b e_x^U(x)\, dx \right\}^{-1}. \qquad (23)$$

Fig. 3 shows the frequency dependence of the characteristic impedances of the symmetrical CPW and slot line. For symmetrical CPW, all three definitions of impedance, (8)–(10), are shown in the figure, while only values based on the power–voltage basis (8) are provided for the slot line case. Both sets of basis functions (13) and (14) have been used for the calculations, but the difference is less than 0.1% for N greater than 8. The frequency dependence of the characteristic impedances of CPW is smaller than that of slot line, and the difference of the values between the definitions (8)–(10) is also small in this case. Frequency-dependent hybrid-mode values converge to the quasi-static values [3] in the lower frequency range for CPW cases, showing the accuracy of the present method.

Transmission line losses are investigated in the following. Total loss (conductor and dielectric) for simple symmetrical CPW is plotted against impedance in Fig. 4(a) together with the published data [10]. A copper conductor is assumed, and its thickness is chosen to be 3 μm [10]. The impedance values are evaluated based on the voltage–current basis (10) and are varied by changing the center strip width, S, while the separation between the grounded conductor, P, is kept constant. The curves of [10] appear to be similar to our results. However, the shape ratio, S/P, which provides the same impedance value, is different from that in [10] (broken lines in

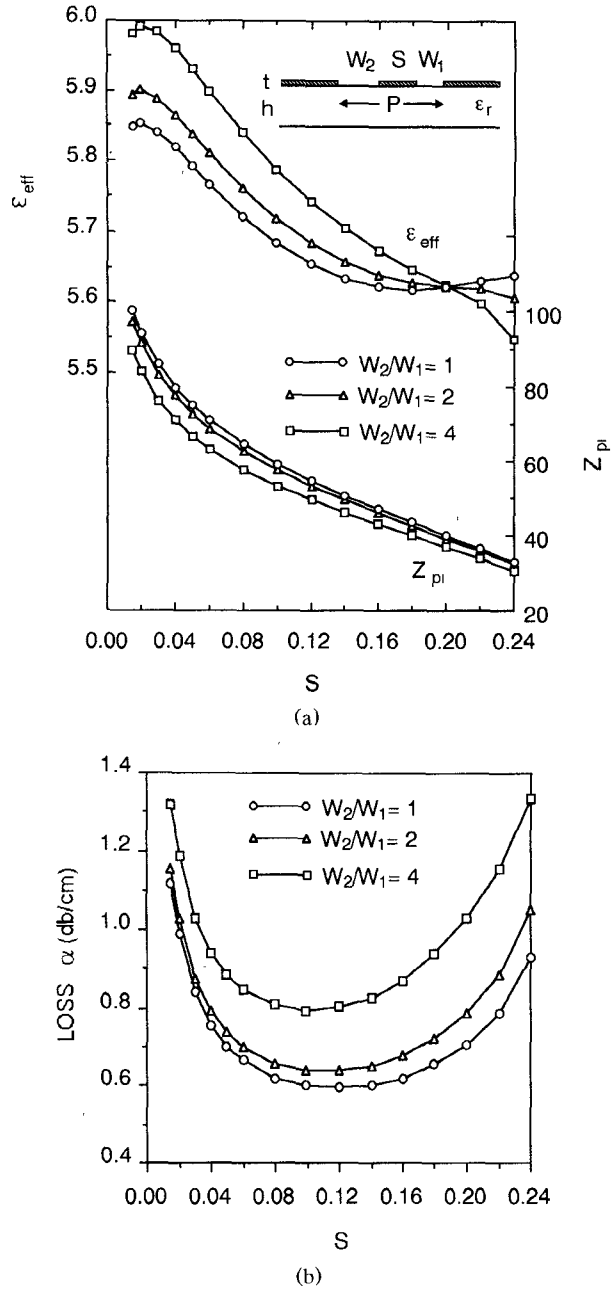

Fig. 7. Propagation characteristics of asymmetrical coplanar waveguide: (a) effective dielectric constant and characteristic impedance of lossless case; (b) attenuation constant. Dielectrics: $\epsilon_r = 12.8$, $\tan\delta = 0.0006$, $h = 0.1$ mm. Conductor: $\rho = 1.7$ $\mu\Omega \cdot$cm, $t = 3$ μm, $P = 0.3$ mm, $f = 60$ GHz.

Fig. 4(a)); that is, the impedance values in [10] are higher than those by the present method (Fig. 4(b)). The metal conductor thickness is neglected in [10], and the total current on the center strip, I_0, in the denominator of (10) does not include the currents on the sidewalls. Also I_0 was calculated by using (21) with $t = 0$, which is relatively sensitive to variations in aperture fields. In Fig. 4(b), the impedance for the zero-thickness case ($t = 0$) is calculated by using (23) with the basis functions of (14) for comparison. When (21) was used instead of (23) for the zero-thickness case and a smaller number of basis functions were used, the present method gave higher value of Z_{VI}.

Fig. 5 shows the frequency-dependent characteristics of symmetrical CPW. Attenuation constants (Fig. 5(b)) show more dispersion than the effective dielectric constants and characteristic impedances (Fig. 5(a)) for CPW.

Parts (a) and (b) of Fig. 6 show the effective dielectric constant, characteristic impedances, and the total transmission line loss for slot line and symmetrical CPW. Equation (14) is used for the impedance calculations both for the slot line and for the CPW in Fig. 6. We mention that the slot line characteristic impedance in Fig. 6(a) is twice that of the CPW for the large center strip width, S, and that the total loss is the same as that of CPW for the large center strip width S (Fig. 6(b)).

Parts (a) and (b) of Fig. 7 show the effective dielectric constant, characteristic impedances, and the total loss for asymmetrical CPW. For the asymmetrical case, the voltage difference between the center strip and the ground conductors is not uniquely specified except at zero frequency [13]. To avoid any ambiguity, we choose the power–current definition (9) here. The parameters are calculated for different values of the slot width ratios W_2 / W_1. The location and width of the center strip are varied such that the separation between the grounded conductor, P, is kept constant. The value S for minimum loss becomes lower with the ratio W_2 / W_1 (Fig. 7(b)) and the impedance value becomes lower with the ratio W_2 / W_1 (Fig. 7(a)); the impedance value for minimum loss then remains about 50 Ω.

VII. Conclusions

Lossy coplanar-type transmission lines have been analyzed by combining the spectral-domain approach with the perturbation method. Introducing a finite thickness of metallization and choosing the proper basis functions for the thick conductor model make the integrals for evaluating the conductor losses remain finite up to the conductor edge without the need to truncate the integrals at a definite distance just short of the edge. Also, the orthogonality relation can be used to reduce the double infinite or semi-infinite integral to the single integral, thereby reducing the computation labor drastically. Numerical computations by new basis functions for the thick conductor show as fast a convergence rate as those for zero-thickness cases. Numerical results include the effective dielectric constants, characteristic impedances, and total losses (conductor and dielectric losses) for slot lines and symmetrical and asymmetrical coplanar waveguides.

References

[1] C. P. Wen, "Coplanar waveguide: A surface strip transmission line suitable for nonreciprocal gyromagnetic device applications," *IEEE Trans. Microwave Theory Tech.*, vol. MTT-17, pp. 1087–1090, Dec. 1969.

[2] T. Kitazawa and Y. Hayashi, "Coupled slots on an anisotropic sapphire substrate," *IEEE Trans. Microwave Theory Tech.*, vol. MTT-29, pp. 1035–1040, Oct. 1981.

[3] T. Kitazawa and R. Mittra, "Quasistatic characteristics of asymmetrical and coupled coplanar-type transmission lines," *IEEE Trans. Microwave Theory Tech.*, vol. MTT-33, pp. 771–778, Sept. 1985.

[4] J. B. Knorr and K. D. Kuchler, "Analysis of coupled slots and coplanar strips on dielectric substrates," *IEEE Trans. Microwave Theory Tech.*, vol. MTT-23, pp. 541–548, July 1975.
[5] T. Kitazawa, Y. Hayashi, and M. Suzuki, "A coplanar waveguide with thick metal-coating," *IEEE Trans. Microwave Theory Tech.*, vol. MTT-24, pp. 604–608, Sept. 1976.
[6] T. Kitazawa and Y. Hayashi, "Quasistatic characteristics of a coplanar waveguide with thick metal coating," *Proc. Inst. Elect. Eng. (Microwaves Antennas & Propagat.)*, vol. 133, no. 1, pp. 18–20, Feb. 1986.
[7] T. Kitazawa and Y. Hayashi, "Quasistatic and hybrid-mode analysis of shielded coplanar waveguide with thick metal coating," *Proc. Inst. Elect. Eng. (Microwaves Antennas & Propagat.)*, vol. 134, no. 3, pp. 321–323, June 1987.
[8] B. E. Spielman, "Dissipation loss effect in isolated and coupled transmission lines," *IEEE Trans. Microwave Theory Tech.*, vol. MTT-25, pp. 648–656, Aug. 1977.
[9] L. Lewin, "A method of avoiding the edge current divergence in perturbation loss calculations," *IEEE Trans. Microwave Theory Tech.*, vol. MTT-32, pp. 717–719, July 1984.
[10] R. W. Jackson, "Considerations in the use of coplanar waveguide for millimeter-wave integrated circuits," *IEEE Trans. Microwave Theory Tech.*, vol. MTT-34, pp. 1450–1456, Dec. 1986.
[11] R. Pregla, "Determination of conductor losses in planar waveguide structures (A comment to some published results for microstrips and microslots)," *IEEE Trans. Microwave Theory Tech.*, vol. MTT-28, pp. 433–434, Apr. 1980.
[12] T. Itoh and R. Mittra, "Spectral-domain approach for calculating the dispersion characteristics of microstrip line," *IEEE Trans. Microwave Theory Tech.*, vol. MTT-21, pp. 496–499, 1973.
[13] T. Kitazawa and T. Itoh, "Asymmetrical coplanar waveguide with finite metallization thickness containing anisotropic media," in *1990 IEEE MTT-S Int. Microwave Symp. Dig.*, pp. 673–676.
[14] R. Mittra and S. W. Lee, *Analytical Techniques in the Theory of Guided Waves*. New York: Macmillan Company, 1971, p. 4.

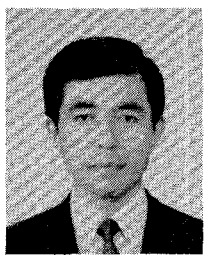

Toshihide Kitazawa (M'84–SM'86) was born in Sapporo, Japan, on December 1, 1949. He received the B.E., M.E., and D.E. degrees in electronics engineering from Hokkaido University, Sapporo, Japan, in 1972, 1974, and 1977, respectively.

He was a Postdoctoral Fellow of the Japan Society for the Promotion of Science from 1979 to 1980. In April 1980, he joined the Kitami Institute of Technology, Kitami, Japan as an Associate Professor of Electronic Engineering. From 1982 to 1984, he was a Visiting Assistant Professor of Electrical Engineering at the University of Illinois, Urbana. From 1989 to 1990, he was a Visiting Scholar of Electrical and Computer Engineering at the University of Texas, Austin. In September 1991, he joined Ibaraki University, Hitachi, Japan, as an Associate Professor of Electrical Engineering.

Dr. Kitazawa is a member of the Information Processing Society of Japan and of the Institute of Electronics, Information and Communication Engineers of Japan.

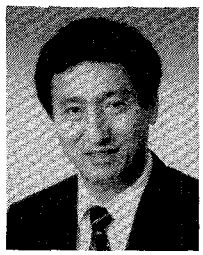

Tatsuo Itoh (S'69–M'69–SM'74–F'82) received the Ph.D. degree in electrical engineering from the University of Illinois, Urbana, in 1969.

From September 1966 to April 1976, he was with the Electrical Engineering Department, University of Illinois. From April 1976 to August 1977, he was a Senior Research Engineer in the Radio Physics Laboratory, SRI International, Menlo Park, CA. From August 1977 to June 1978, he was an Associate Professor at the University of Kentucky, Lexington. In July 1978, he joined the faculty at the University of Texas at Austin, where he became a Professor of Electrical Engineering in 1981 and Director of the Electrical Engineering Research Laboratory in 1984. During the summer of 1979, he was a Guest Researcher at AEG-Telefunken, Ulm, Germany. In September 1983, he was selected to hold the Hayden Head Centennial Professorship of Engineering at the University of Texas. In September 1984, he was appointed Associate Chairman for Research and Planning of the Electrical and Computer Engineering Department at the University of Texas. In January 1991, he joined the University of California, Los Angeles, as Professor of Electrical Engineering and holder of the TRW Endowed Chair in Microwave and Millimeter Wave Electronics.

Dr. Itoh is member of the Institute of Electronics and Communication Engineers of Japan, Sigma Xi, and Commissions B and D of USNC/URSI. He served as the Editor of the IEEE TRANSACTIONS ON MICROWAVE THEORY AND TECHNIQUES for the years 1983–1985. He serves on the Administrative Committee of the IEEE Microwave Theory and Techniques Society. He was Vice President of the Microwave Theory and Techniques Society in 1989 and President in 1990. He is Editor-in-Chief of the IEEE MICROWAVE AND GUIDED WAVE LETTERS. He was Chairman of USNC/URSI Commission D from 1988 to 1990 and is Vice Chairman of Commission D of the International URSI. Dr. Itoh is a Professional Engineer registered in the state of Texas.